Sulfation of furcellaran and its effect on hemocompatibility in vitro

Sulfation of furcellaran and its effect on hemocompatibility in vitro

Kateřina Stěpánková[a], Kadir Ozaltin[a], Radka Gorejová[a,b], Hana Doudová[a], Eva Domincová Bergerová[a], Iveta Maskalová[c], Monika Stupavská[d], Pavel Sťahel[d], David Trunec[d], Jana Pelková[e,f], Miran Mozetič[g], Marian Lehocky[a,*]

[a]*Centre of Polymer Systems, University Institute, Tomas Bata University in Zlín, Trida Tomase Bati 5678, 760 01 Zlin, Czech Republic*

[b]*Department of Physical Chemistry, Faculty of Science, Pavol Jozef Šafárik University in Košice, Moyzesova 11, 041 54 Košice, Slovakia*

[c]*Department of Animal Nutrition and Husbandry, University of Veterinary Medicine and Pharmacy in Kosice, Slovakia*

[d]*Department of Physical Electronics, Faculty of Science, Masaryk University, Kotlářská 2, 611 37 Brno, Czech Republic*

[e]*Department of Hematology, Tomas Bata Regional Hospital, Havlickovo Nabrezi 2916, 76001 Zlín, Czech Republic*

[f]*Faculty of Humanities, Tomas Bata University in Zlín, Stefanikova 5670, 76001 Zlin, Czech Republic*

[g]*Department of Surface Engineering Jozef Stefan Institute, Jamova cesta 39, 1000 Ljubljana, Slovenia*

[*]*Corresponding author. E-mail addresses: k1_stepankova@utb.cz (K. ětěpánková), ozaltin@utb.cz (K. Ozaltin), radka.gorejova@upjs.sk (R. Gorejová), h1_doudova@utb.cz (H. Doudova), iveta.maskalova@uvlf.sk (I. Maskalova), pstahel@physics.muni.cz (P. Sťahel), trunec@physics.muni.cz (D. Trunec), pelkova@utb.cz (J. Pelková), miran.mozetic@ ijs.si (M. Mozetic), lehocky@utb.cz (M. Lehocky).*

ABSTRACT

In this study, furcellaran (FUR) obtained from Furcellaria lumbricalis was firstly employed for sulfation via various methods, including SO_3-pyridine (SO_3•Py) complex in different aprotic solvents, chlorosulfonic acid and sulfuric acid with a "coupling" reagent N,N'-Dicyclohexylcarbodiimide. Structural characterization through $FT-IR$, GPC, XPS and elemental analyses confirmed the successful synthesis of 6-O-sulfated FUR derivates characterized by varying degrees of sulfation (DS) ranging from 0.15 to 0.91 and molecular weight (M_w) spanning from12.5 kDa to 2.7 kDa. In vitro clotting assays, partial thromboplastin time ($aPTT$), thrombin time (TT), and prothrombin time (PT) underscored the essential role of sulfate esters in conferring anticoagulant activity whereas FUR prepared via chlorosulfonic acid with DS of 0.91 reached 311.4 s in $aPPT$ showing almost 4-fold higher anticoagulant activity than native FUR at the concentration 2 mg/mL. MTT test showed all tested samples decreased cell viability in a dose dependent manner while all of them are non-cytotoxic up to the concentration of 0.1 mg/ mL. Furthermore, sulfated derivates deposited onto polyethylene terephthalate surface presented substantial decrease in platelet adhesion, as well as absence of the

most activated platelet stages. These findings support the pivotal role of O-6 FUR sulfates in enhancing hemocompatibility and provide valuable insights for a comparative assessment of effective sulfating approaches.

Keywords: Furcellaran, seaweed polysaccharide, sulfation, anticoagulant, platelet adhesion. Hemocompatibility

1. Introduction

Venous or arterial blood clots can lead to venous thromboembolism or acute coronary syndrome and have been reported as the third leading cardiovascular diagnosis [**1**]. As is known, unfractionated (UFH) and low-molecular-weight ($LMWHs$) heparins have been the predominant anticoagulant and antithrombotic drugs used in a clinical practice [**2**]. The potent anticoagulant action of heparin is achieved mainly through potentiation of antithrombin and heparin cofactor II, the major inhibitors of coagulation enzymes, in particular thrombin and factor Xa. The heparin minimal pentasaccharide sequence with sulfate pattern at specific positions is required to induce an activating conformational change in antithrombin [**3,4**]. The low $LMWHs$ heparin is currently an alternative for the treatment of prophylaxis against thromboembolic disorders because of its longer half-life in blood circulation system, higher bioavailability and lower variability in coagulation response [**5**]. However, it has certain limitations, including thrombocytopenia, haemorrhage, congenital or acquired antithrombin deficiency invalidation and risk of animal pathogen contamination due to its animal origin [**6,7**]. Therefore, it is crucial to search for alternative sources of anticoagulant agents which do not compromise patient health.

In recent years, there has been increasing interest in the utilization of plant polysaccharides as a renewable, non-animal source of heparin analogues. Seaweed polysaccharides have gained attention due to their abundant marine storage and properties like biocompatibility, biodegradability and non-toxicity [**8**]. Various sulfated polysaccharides (SP) from red and brown algae have been reported to exhibit anticoagulant, antithrombotic, fibrinolytic, and platelet-aggregating effects. Specifically, these biological effects have been attributed to the structural compounds of sulfated galactans and sulfated fucans, respectively. All these activities are closely associated with the presence of hemiester sulfate groups, which play a paramount role in molecular recognition, cell development, and cell-cell interactions [**9-12**]. Focusing on gal-actans, other diverse biological properties were exhibited. Among them, it can be highlighted antitumor [**13**], antiviral [**14**], antioxidant [**15**], antinociceptive [**16**], anti-inflammatory [**17**] and pro-inflammatory [**18**]. These evidences are the main reasons for the increase of studies with this group of molecules and their eligible use in medical and pharmaceutical applications. With its anionic structure enabling efficient chelation of cationic dyes and heavy metals, SPs provide an environmental advantage as highly effective adsorbents for removing organic dyes and toxic metal pollutants from wastewater, which has become a global concern [**19-21**].

Furcellaran is a naturally sulfated anionic galactan isolated from the red algae (Furcellaria lumbricalis). The species is widespread in the North Atlantic and brackish waters of the Baltic sea. The current abundance of loose-lying $F.$ lumbricalis in Estonia is considered as the greatest in the world, where besides manufacturing, technology is being actively developed in order to improve the quality of production [**22**], as the production volume is currently marginal compared to other major producers of seaweed polysaccharides. Each year, the total amount of biomass fluctuates, but it typically falls between 100,000 and 200,000 tons based on wet weight. The majority, ranging from 60 % to 73 %, is

attributed to F. lumbricalis [23]. Furcellaran is structurally and functionally similar to K-carrageenan but differs in the number of sulfate esters. It consists of repeating backbone of alternating (1 → 4)-3,6-anhydro-$a-_D$-galactopyranose-(1 → 3)-$\beta-_D$-galactopyranose-4'-sulfate structural units with approximately one sulfate ester per three monomer residues [**24**]. The most important property of furcellaran is its gelforming ability, which involves the random coil to helix transition upon cooling, followed by the cation-specific aggregation of helices with subsequent gel formation [**25**]. For this reason, furcellaran is currently applied as a gelling-stabilizing agent in food processing [**26**], as a component for the development of edible films and coatings [**27**] as well as multilayer capsules for drug delivery [**28**]. Recently, it has been proposed as a natural material for use in the biomedical field [**29**].

Several studies have shown that native polysaccharides exhibit only weak bioactivities, which may be greatly enhanced by molecular modification [**30**]. Chemical modifications, such as sulfation, provide an effective approach to overcome the poor water solubility and improve the bioactivity of natural polysaccharides by altering their structural and conformational properties [**31-33**]. Many recent evidences indicate that besides the density of polyanionic charges, some structural factors such as glycoside linkage configuration, molecular weight and the position of sulfate esters in the polymer chain can influence the potential bioactive properties [**34-36**]. These structural features can be affected by the sulfation method which can vary in terms of the sulfating agent, medium, reaction time, temperature and molar ratios of the reaction components. Yang et al. reported that the optimal conditions for obtaining Chinese laquer polysaccharides with high DS and Mw include maintaining a temperature range of 40-80 °C with 4:1 M ratio of SO_3-Py complex to sugar unit and reaction time for 3 h, respectively [**37**]. K-carrageenan and agarose with chlorosulfonic acid-pyridine method, whereas the optimal reaction condition was determine through reaction time of 4 h, the reaction temperature 65 °C, and the ratio of chlor-osulfonic acid and polysaccharide was 1-4 (mL/g) [**38,39**]. Chlor-osulfonic acid, anhydrous sulfuric acid, and complexes of SO_3 with pyridine are the most commonly used sulfating agents. The reaction is usually performed in aprotic solvents such as dimethylformamide (DMF), dimethyl sulfoxide ($DMSO$) or pyridine [**30,40**]. Nevertheless, due to the structural complexity of polysaccharides, a sulfation method that resulted in predictable derivatives of a particular polysaccharide was not readily applicable to another polymer. For instance, β-(1 → 6)-d-Glucans [**41**], glycoglucuronomannan [**42**] and mannogalactan [**43**] have been sulfated with excess of $ClSO_3H$. Conversely, polysaccharides from starch, glucans [**44**], polysaccharides from fruiting bodies [**45**] and fucans [**46**] have been sulfated through excess of SO_3-pyridine complex. Starch, agarose, K-carrageenan were sulfated by sulfuric acid with dicyclohexylcarbodiimide (DCC) [**47**]. Sulfation is usually carried out under non-regioselective conditions, resulting in randomly distributed sulfate groups along the polymer chain. Reports on the oversulfation of the main types of carrageenans manifest the major substitution on G-6 position [**39,48**]. Regioselective insertion of sulfate esters at specific positions and selective modification of the sulfation pattern in native carrageenans have also been published [**36**].

We have already conducted a comparative study of furcellaran with K-carrageenan [**29**], which have been extensively investigated due to their commercial importance and widespread use in various industries. As mentioned above, its sulfation pattern is the major contributor to its bioactivity and the main difference compared to furcellaran. Many types of chemical modifications have been already accomplished with K-carrageenan. However, to date, there are no studies devoted to sulfated modification of furcellaran that may have functional and medicinal value. The development of new heparinoids, particularly those of plant origin, carries paramount importance in various medical applications (i.e., anticoagulant therapy, coatings of stents, catheters or other blood contacting devices, and inclusion in drug delivery systems [**49,50**]. The exploration of furcellaran within this

context emerges as a promising avenue for these potential applications. Therefore, the main objective of this study is of sulfating approaches with aim to enhance hemocompatibility of furcellaran. Various sulfating agents that were chosen based on their established track record in the literature as well as their availability, ensuring consistency and comparability with earlier studies of other galactans [**36,39,51**]. Subsequently, the potential improvement in hemocompatibility was investigated. Structural characterization was analyzed by Fourier-transform infrared spectroscopy ($FT-IR$), X-ray photoelectron spectroscopy (XPS) and gel permeation chromatography (GPC). Platelet poor plasma was used to measure activated partial thromboplastin time ($APPT$), thrombin time (TT) and prothrombin time (PT) to assess the anticoagulant activity in vitro. Complementary to that, platelet-rich plasma was used to evaluate a possible antithrombotic effect via the platelet adhesion test, and the MTT assay was performed to determine cytotoxicity of tested samples.

2. Materials and methods

2.1. Materials and reagents

Furcellaran (FUR) Estgel 1000 [FB; M_w 2.55 × 10^5 Da; water gel strength of Bloom 480 g (2.5 % furcellaran; trigger 4.5 g, deformation 15.0 mm and speed 0.4 mm × s^{-1}); pH 8.30 (1.0 % aqueous solution at 25 °C); and 9.7 % moisture] was obtained from Est-agar a.s. (Kärla village, Estonia) and was used without further purification. Strong acid cation exchanger, Amberlite® IR-120, H^+, Dialysis sacks (molecular weight cut-off ($MWCO$), 12,000 Da) and Pyridine - anhydrous, 99.9 % were purchased from Sigma-Aldrich (St. Louis, MO, USA) and used for the conversion to pyridinium salt. N, N-Dimethylformamide - anhydrous, 99.8 % (Thermo Fisher Scientific, Waltham, MA, USA), Sulfuric acid 96 % (Penta, Prague, Czech Republic) N,N'-Dicyclohex-ylcarbodiimide ≥99 % (Fluka Analytical, Charlotte, NC, USA), Dimethyl Sulfoxide ($DMSO$) - anhydrous, 99.9 % (Sigma-Aldrich, St. Louis, MO, USA), Chlorosulfonic acid (Sigma-Aldrich (St. Louis, MO, USA) and Sulfur trioxide pyridine complex (Sigma-Aldrich (St. Louis, MO, USA) were employed in the synthesis of sulfated derivates. Heparin sodium salt from porcine intestinal mucosa ≥180 USP units/mg (Sigma-Aldrich (St. Louis, MO, USA) was used for anticoagulant analysis. All reagents were analytical grade unless otherwise stated.

2.2. Furcellaran pyridinium salt

An aqueous solution of furcellaran (1 g/L) as Na^+ salt was passed through a cation-exchange column of Amberlite IR 120$^+$ (H^+) and the eluate was adjusted to pH 7-8 by addition of the anhydrous pyridine. The obtained solution was dialyzed ($MWCO$ 12,000) via $DEMI$ water for 72 h. Subsequently, the solution was casted in a glass mold and frozen at —18 °C for 24 h followed by lyophilization at —110 °C of freeze-drying and pressure 0.2 mbar (CoolSafe 110-4 Pro, Scanvac, Lynge, Denmark) for 48 h. The resulting pyridinium salt of the SP (**Fig. 1**a) was over-sulfated by different approaches as described below.

2.3. Sulfation methods

2.3.1. Sulfur trioxide pyridine method

The freeze dried pyridinium salt of furcellaran (200 mg) was dissolved in 30 mL anhydrous $DMSO$ by stirring at room temperature for 30 min, and then SO_3•Py complex in molar ratio 4:1 to sugar units were separately added. The mixture was heated in an oil bath at 70 °C and stirred under nitrogen

atmosphere for 3 h. The reaction mixture was poured into ice water and neutralized with 1 M NaOH solution to the value (pH 7-8) and precipitated with 75 % ethanol. The precipitate was dialyzed for 72 h against 5 L of demineralized water and lyophilized to give sample FUR_DMSO (**Fig. 1**b). The same procedure was performed with the difference of using anhydrous DMF as a solvent to give sample FUR_DMF (**Fig. 1**c).

2.3.2. Chlorosulfonic method

Anhydrous DMF (30 mL) was added to a 250 mL three-necked flask equipped with a thermometer, drying tube and rubber stopper. Then, 2 mL of chlorosulfonic acid was added dropwise under agitation and with cooling (—5 °C to 0 °C) to form the SO_3•DMF complex. After the reaction was completed, furcellaran (200 mg) was added and the reaction mixture was heated at 60 ° C during 2 h under nitrogen atmosphere. The resulting solution was cooled down, neutralized and precipitated by 75 % ethanol. The precipitate as previously was purified by dialysis for 3 days and the final product was freeze-dried to give sample FUR_HSO3CL (**Fig. 1**d).

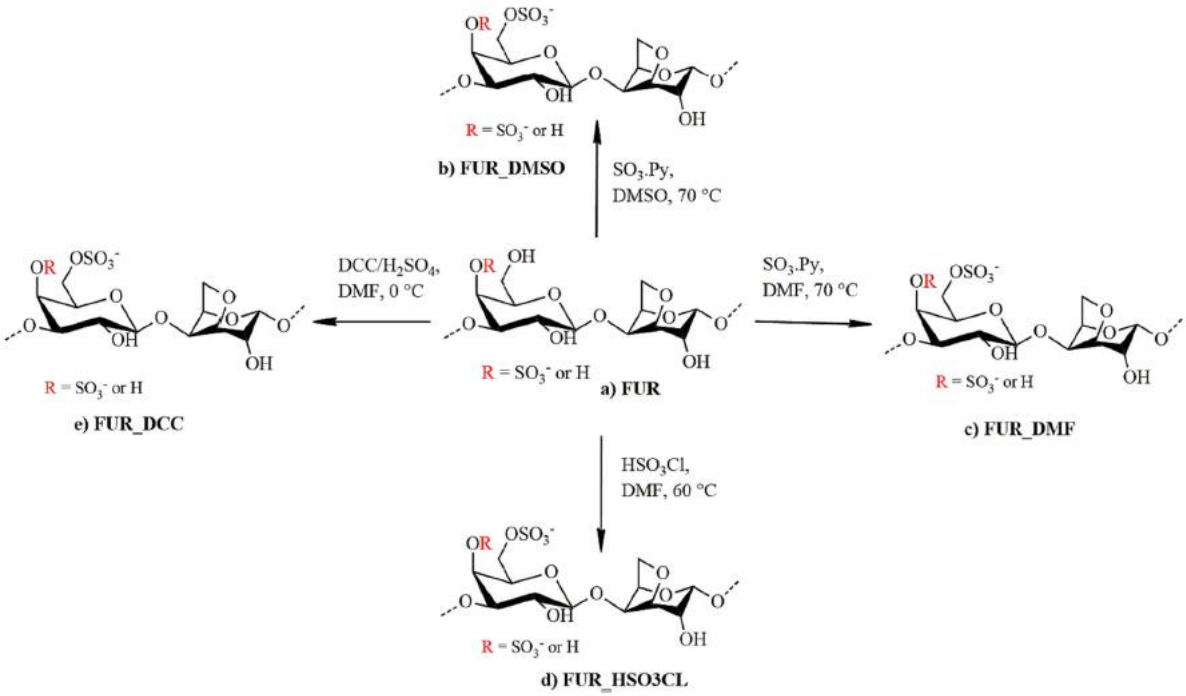

Fig. 1. Reaction scheme of the a) furcellaran sulfation by different approaches. According to reaction agent SO_3•Py complex and as medium dimethyl sulfoxide b) FUR_DMSO or dimethylformamide c) FUR_DMF, via chlorosulfonic acid d) FUR_HSO3CL and with a coupling agent dicyclohexylcarbodiimide/H_2SO_4 e) FUR_DCC.

2.3.3. Sulfation with sulfuric acid mediated by dicyclohexylcarbodiimide

Sulfation was carried out according to Takano et al. [**47**] Briefly, furcellaran (400 mg) was dissolved in anhydrous DMF (20 mL) and to this mixture was added DCC (800 mg) dissolved in DMF (20 mL). The solution was cooled down to 0 °C and 150 pL of 96 % H_2SO_4 was added dropwise. The reaction mixture was maintained at 0 ° C for 30 min under nitrogen stream. The resulting mixture was poured into crushed ice (100 g), immediately neutralized with 1 M NaOH and filtered with Celite 500 to remove dicyclohexylurea formed from DCC. Subsequently, the fractions containing furcellaran with sulfate

esters were collected, dialyzed against $DEMI$ water for 3 days and lyophilized to give sample FUR_DCC (**Fig. 1**e).

2.4. $FT-IR$, GPC, XPS structural analysis

The $FT-IR$ spectra of the native and sulfated furcellaran samples were recorded using a Nicolet iS5 (Thermo Scientific, Grand Island, NY, USA) single beam Fourier transform infrared spectroscopy ($FT-IR$) equipped with iD5 attenuated total reflectance (ATR). Collected spectra were recorded between 600 and 4000 cm^{-1} with a resolution of 2 cm^{-1} and 64 scans using a germanium crystal at an incident angle of 45°.

Initially, furcellaran sulfates samples' molecular weight distribution was analyzed by the gel permeation chromatography (GPC), a type of size-exclusion chromatography employing conventional calibration, using a Waters HPLC Breeze chromatographic system set up with a Tosoh TSK gel GMPWXL column (300 mm × 7.8 mm × 13 μm, column T = 30 °C) (Tosoh, Tokyo, Japan) and a Waters 2414 refractive index detector (drift tube T = 60 °C) (Waters, Milford, MA, USA). A mixture of 0.1 M $NaNO_3$ and 0.05 M $Na_2HPO_4{\cdot}12H_2O$ was employed as a mobile phase. Calibration was carried out using pullulan polysaccharide calibration kit SAC-10 (Agilent Technologies, Santa Clara, CA, USA) in a span of M_w 342-708,000 g/mol.

To analyze the change of chemical composition on the furcellaran surfaces and chemical binding state, X-ray Photoelectron Spectroscopy (XPS) was used. The XPS measurements were performed using the ESCALAB 250Xi device (Thermo Fisher Scientific, East Grinstead, United Kingdom). An X-ray beam with power of 200 W (650 μm spot size) was used. The survey spectra were acquired with a pass energy of 50 eV and energy step of 1 eV. High-resolution scans were acquired with a pass energy of 20 eV and energy step of 0.1 eV. In order to compensate for charges on the surface, an electron flood gun was used. Spectra were referenced to the hydrocarbon type C 1s component set at a binding energy of 284.8 eV. Spectra calibration, processing and fitting routines were done using the Avantage software.

2.5. Elemental analysis and degree of sulfation

Elemental analysis (carbon, hydrogen, nitrogen, and sulfur) was performed by organic elemental analyzer (FLASH 2000 CHNS/O + MAS200R, Thermo Fisher Scientific, Sunnyvale, CA USA). The percentage of sulfur (% S) and carbon (% C) were used to calculate the degree of substitution (DS) according to the formula (Eq. (**1**)) [**52,53**]:

$$\mathrm{DS} = 2.25 \times (\mathrm{S\%}/\mathrm{C\%}) \qquad (1)$$

The percentage yield of FUR and its sulfated derivates as given in Eq. (**2**) [**54**].

$$\mathrm{Yield}\ (\%) = \frac{\mathrm{W1}}{\mathrm{W0}} \times 100 \qquad (2)$$

Where w_1 = weight of FUR and w_0 = weight of furcellaran sulfates.

2.6. Evaluation of anticoagulant aktivity

The prothrombin time (PT), thrombin time (TT) and activated partial thromboplastin time ($aPTT$) tests were used for determination of anticoagulant activity in vitro. The blood was obtained by venous puncture from a healthy donor in accordance with the Helsinki Declaration, and placed into blood collection tubes (VACUETTE, Greiner Bio-One, Kremsmunster, Austria). The obtained human blood plasma was treated with 3.2 % citric acid (109 mmol/L) and then centrifuged at room temperature, 3000 rpm, for 15 min. The polysaccharide samples were dissolved in saline solution (0.9 %) to form different concentrations: 0.1, 0.5, 1, and 2 mg/mL. 125 μL furcellaran sample solution was placed into each plastic tube followed by addition of 250 μL plasma. Final concentration corresponds to 0.033, 0.166, 0.333, and 0.666 mg/ mL, respectively, in the experimental system. The clotting time was measured by automatic coagulation analyzer SYSMEX CA-1500 (Siemens, Munich, Germany). The principle of the measurement is based on monitoring changes in turbidity at 660 nm as consequence of adding coagulation reagent which induces the formation of fibrin clots. For each experimental group, $n = 3$ independent samples were used, and each of the sample was analyzed in triplicate.

2.7. In vitro fibroblast cytocompatibility

The cytotoxicity of furcellaran and its derivates was tested using the mouse embryonic fibroblast cell line (NIH/3 T3, ATCC® CRL-1658TM, Manassas, VA, USA) according to EN ISO 10993-5. Firstly, the tested samples were dissolved in water with a concentration of 2 mg/mL and subsequently sterilized with a filter syringe (0.22 μm pore size). Sterilized sample solutions were then diluted in culture medium to obtain 50, 25 and 5 % concentrations. The ATCC-formulated Dulbecco's modified Eagle's medium (BioSera, Nuaille, France) containing 10 % calf serum (BioSera, Nuaille, France) and 100 U mL^{-1} penicillin/streptomycin (BioSera, Nuaille, France) was used as the culture medium. The cells were pre-cultivated in a 96 well plate at the concentration of 1×10^5 cells per mm^2 at 37 ± 1 °C for 24 h. After the incubation the cell medium was replaced by prepared sample solutions for another 24 h. After 48 h of cell culturing, the cell viability was evaluated using the 3-(4,5-Dimethylthiazol-2-yl)-2,5-diphenyltetrazolium bromide (MTT) assay (Duchefa Biochemie, Amsterdam, the Netherlands). Firstly, the culture medium was removed and 100 μL of growth medium containing MTT dye solution (5 mg/mL in PBS) was added to the cultures. Then, cells were incubated at 37 °C in humidified atmosphere for 4 h. Following the removal of growth medium, DMSO (Sigma-Aldrich, St. Louis, MO, USA) was added to dissolve the formed formazan crystals on the sample surface. The absorbance was measured by an Infinite M200 Pro NanoQuant absorbance reader (Tecan, Mannedorf, Switzerland) at a wavelength of 570 nm (test) and 690 nm (reference). Reported values are the means of three replicates and are expressed as percentages of control (polystyrene) value.

2.8. Platelet adhesion test

Prior to testing, the furcellaran and its sulfated derivates were immobilized onto polyethylene terephthalate (PET) films according to method of Ozaltin et al. [**55**] with minor modifications. Briefly, circular PET films ($d = 30$ mm) were treated by low pressure plasma equipment (Diener Electronic, Nagold, Germany) to introduce functional groups for further covalent bonding. Subsequently, the PET films were immersed into 0.1 % (w/v) polysaccharide solution for 24 h at room temperature. After the

deposition, the samples were taken out of the solution, washed in distilled water and dried overnight at 25 °C.

Platelet-rich plasma (PRP) was obtained from the upper fluid of whole blood by centrifugation at 1000 rpm for 10 min. The samples were disinfected by germicidal UV light for 20 min and then transferred to 24-well plates. 200 μL of PRP was added to each well and left to incubate at 37 °C for 1 h. Samples then were rinsed by PBS to remove non-adherent platelets, and 2.5 % glutaraldehyde solution was used to fix adhered platelets on the bulk sample surface at room temperature for 1 h. To dehydrate the platelets, different gradient ethanol solutions (50 %, 60 %, 70 %, 80 %, 90 %, and 100 % vol% with water) were used (each concentration for 10 min) at 4 °C and then freeze-dried for 4 days. The morphology of the adhered platelets was observed by scanning electron microscope (SEM) coupled with the energy dispersive spectrometer (EDX) (JEOL JSM-7000F, with $EDX\ INCA$ analyzer, Akishima, Japan).

2.9. Statistical analysis

All experimental analysis for anticoagulant and cytotoxicity evaluations were performed in triplicate ($n = 3$ for each experimental value). The data were represented as mean $\pm$ standard deviation (SD). Two-way ANOVA (analysis of variance) followed by Bonferroni post-hoc test was used for data evaluation and $p < 0.05$ was accepted as statistically significant. Statistical analysis was performed using GraphPad Prism® 5.0 (GraphPad Software Inc., La Jolla, CA, USA).

3. Results and discussion

3.1. $FT-IR$ spectroscopy

$FT-IR$ spectroscopy was used in order to characterize native furcel-laran and its sulfated derivates. Obtained $FT-IR$ spectra are shown in **Fig. 1**. The O—H stretching signal is observed at around 3400 cm^{-1}, asymmetric C—H stretch band of the saccharide ring at 2920 cm^{-1} and band 1650 cm^{-1} can be attributed to water deformation [**39,56,57**]. For native furcellaran (**Fig. 2**, spectrum (a)) one band occurs at 845 cm^{-1} corresponding to the axial galactose-4-sulfate [**58,59**]. After sulfation, the absorption band appeared at 820 cm^{-1} (**Fig. 2** (b)-(e)) which can be assigned to C-O-S of galactose-6-sulfate [**18**] and peak arising from galactose-4-sulfate was obscured. This might be due to lability of polysaccharide towards to the sulfation methods used. According to previous study, one contributing factor to the desulfation of polysaccharides is their subjection to high-temperature solvolysis in an aprotic solvent containing trace amounts of water or methanol this process results in extensive depolymerization and absence of selectivity in sulfate group cleavage sites [**40**]. For the FUR_DCC (**Fig. 2**, spectrum (e).), sulfated groups were proportionally distributed to G4 and G6 positions. However, the intensity of bands was negligible compared to other samples. Generally, chemical sulfation promotes partial cleavage, reducing the M_w of the resulting polymer. Since 3,6-anhydro-a-gal-actosidic bond in the structure of furcellaran is easily destroyed by acidic conditions, its existence is closely related to depolymerization [**60**]. The presence of 3,6-anhydro-galactosidic bond is confirmed by band at 930 cm^{-1} in all sulfated samples [**39**]. Nevertheless, band intensity is lower compared to native furcellaran. The sample FUR_HSO3CL (spectrum (d)) exhibited the least intense band indicating a partial disruption of galactosidic bond. Band at 1060 cm^{-1} is attributed to C—O stretching vibration of sulfate ester groups. The most intense band is found at 1220 cm^{-1} indicating total sulfate content [**61**].

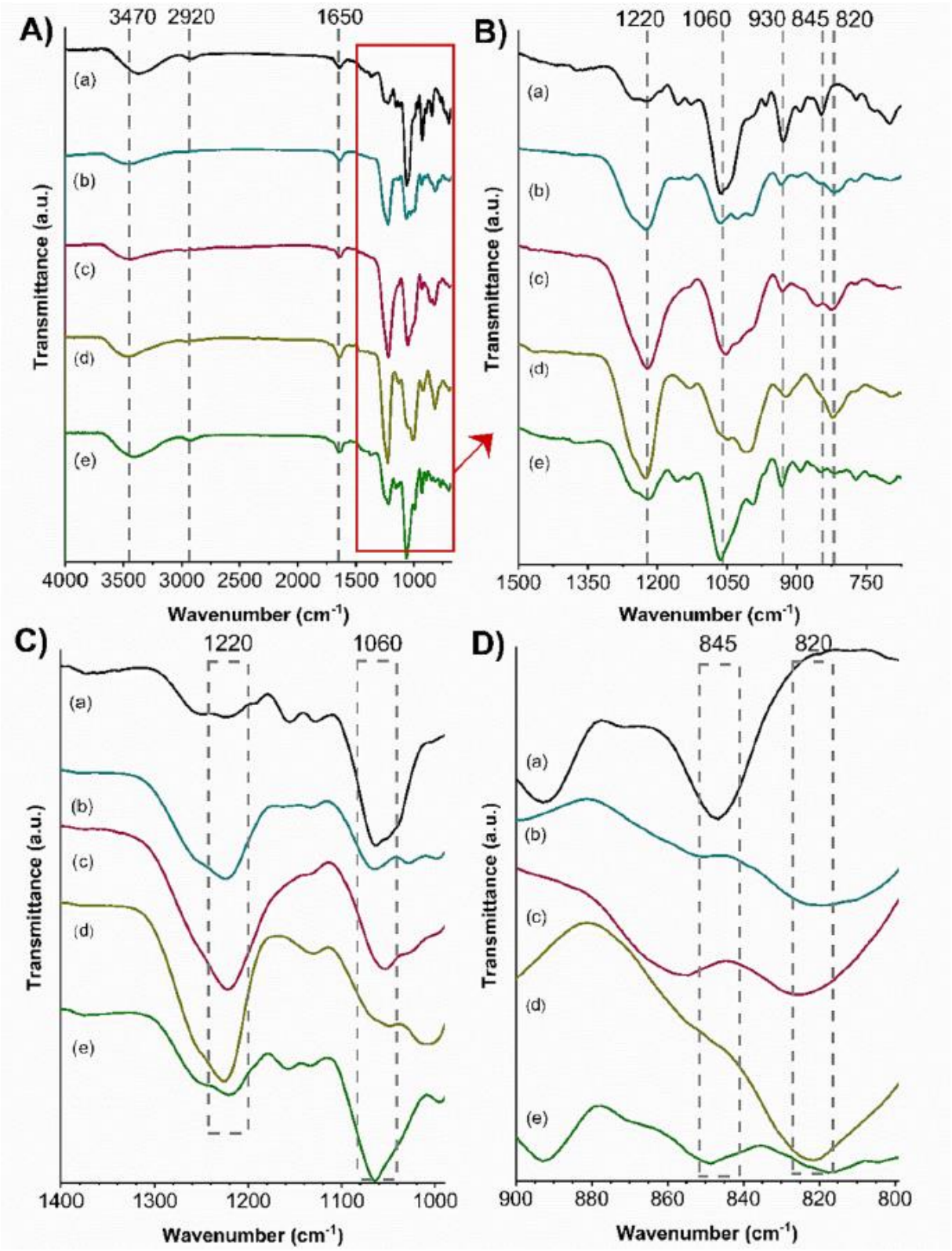

Fig. 2. Attenuated total reflectance $(ATR) - FT - IR$ spectrum collected from the samples: A) (a) is for FUR, spectrum (b) is for FUR_DMSO, spectrum (c) is for FUR_DMF, spectrum (d) is for FUR_HSO3CL and spectrum (e) is for FUR_DCC. B) characteristic absorption bands in the range 1300-790 cm^{-1}. C) detail of the 1220 cm^{-1} and 1060 cm^{-1} of samples. D) detail of the 845 cm^{-1} and 820 cm^{-1} of samples.

3.2. Molecular weight distribution

To investigate the dependence of the varied synthesis strategies on the FUR molecular weight distribution, all prepared FUR samples were analyzed using GPC with pullulan standards; the detailed results, including weight- and number-averaged molecular weights (M_w and M_n, respectively) as well as their polydispersity (as $M_w/\ M_n$ ratio) are summarized in **Table 1**. Results demonstrate the high polydispersity index (PDI) of furcellaran pyridinium salt. This could be linked to several factors, including the process of isolation and purification, which may affect the polymer's molecular weight distribution. Furthermore, the inherent polydispersity of the native furcellaran polymer may have contributed to the observed result.

Table 1 Molecular weight (M_w) of furcellaran and its derivates.

Sample	M_w (Da)[b]	M_n(Da)[c]	PDI[d]
FUR[a]	131,534	2276	57.80
FUR_DMSO	12,473	3640	3.43
FUR_DMF	7648	2751	2.78
FUR_HSO3CL	2720	1078	2.52
FUR_DCC	4816	1414	3.40

[a] Furcellaran in the pyridinium salt form. [b] M_w - molecular weight. [c] Mn - average molecular weight. [d] PDI - polydispersity index.

It should be noted that certain disaccharides, such as sucrose, which may be present in native furcellaran, could potentially contribute to the higher polydispersity as well. After sulfation, a significant decrease in PDI was observed, which could be attributed to the removal of low molecular weight impurities through precipitation, dialysis and sulfation itself. Mw of oversulfated derivatives ranged from 12,473 Da to 2720 Da. Compared to FUR, a notable decrease in Mw was observed in all sulfated samples. Sulfating agents such as chlorosulfonic acid or sulfuric acid degraded the polysaccharide during sulfation most likely in a radical mechanism. Due to their hygroscopicity, these reagents with very high reactivity may lead to undesirable hydrolysis in acidic environment and partial destruction of furcellaran backbone. These results are consistent with previous reports [**45,62**]. For instance, sulfation of agarose via chlorosulfonic acid resulted in degree of substitution (DS) of 0.91 and showed a reduction of up to half of its original molecular weight [**38**]. In contrast, mildly acidic character of the SO_3•Py complex manifested in a higher M_w, however an extensive degradation during the reaction was also accompanied. Besides the molar ratio of reagent to sugar unit used, the major factor resulting in the degradation is temperature and reaction time [**37**]. It was also reported, that certain protecting groups, for example trime-thylsilyl, may protect polysaccharide from degradation in the course of sulfation procedure [**36,63**]. In order to maintain the macromolecular features of the native furcellaran during the sulfation, optimum conditions (temperature, reaction time and molar ratios of reagent) are required.

3.3. XPS

A considerably better detection of chemical structure is provided by the XPS technique that analyzes surface layers of a thickness up to 10 nm. **Table 2**. presents the atomic concentration of elements for furcellaran and its derivates. **Table 2** shows only selected elements of interest - C, O, S, the

characteristic components of furcellaran. XPS analysis also revealed a low amount (≤3 %) of Na, K, N, Si and traces (<1 %) of Ca and Mg on the surface of studied samples.

The chemical composition and the binding state of the furcellaran and its derivates were compared using the curve fitting of the high-resolution C 1s peak.

Table 2 Chemical composition (%) and relative peak area (%) of carbon chemical bonds for furcellaran samples.

Sample	C	O	S	C-C/ C-H	C-S	C-O	C=O	COO
FUR	59 ± 3	38 ± 4	2 ± 1	22	1	59	15	3
FUR_DMSO	48 ± 2	41 ± 2	7 ± 1	21	11	54	12	2
FUR_DMF	60 ± 3	32 ± 4	5 ± 1	31	24	33	9	3
FUR_HSO3CL	52 ± 3	34 ± 2	6 ± 1	32	25	31	9	3
FUR_DCC	52 ± 5	42 ± 2	4 ± 1	13	4	58	22	3

Fig. 3a) shows the comparison of the full shape of carbon peaks for all studied samples. Inset displays the deconvolution of C 1s peak for FUR sample. The C 1s peak is deconvoluted into five components, located at ~284.6, ~285.0, ~286.3, ~287.8 and ~289.0 eV, respectively. The component at ~284.6 eV can be assigned to hydrocarbon $C-C/C-H$ bonds, and component at 285.0 eV to $C—S$ chemical bonds. As seen in **Fig. 3**b), all samples exhibited sulfur peak S2p3/2 located in the spectrum at 167,7 eV, which is a characteristic bond energy for sulfate group. The binding capacity of sulfur did not change in any way by changing the reaction conditions.

The components centered at a binding energy ~286.3 eV, 287.8 eV and ~289.0 eV can be attributed to oxygen - containing functional groups, $C—O$, $C-O$ and $O-C=O$, respectively. $C-O$ group may indicate the process of polysaccharide oxidation. This might be due to alkali treatment of furcellaran during the extraction, which is applied to improve furcellaran gelling ability by removing sulfates and forming 3,6-anhydrogalactose [**24**]. Other factors might be attributed to storage, handling and reaction conditions. It should be noted, that sulfates when exposed to air or moisture readily decompose, resulting in the production of sulfuric acid and cleavage of carbohydrate chain length.

Results of deconvolution are summarized in **Table 2**. The decomposition is validated by good agreement with elemental composition, where similarly to $C—S$ behavior; the concentration of sulfur shows the same trend.

Elemental analysis (**Table 3**.) confirmed that the parental polysaccharide has low sulfur content detected, whereas for the oversulfated samples the sulfur was increased.

3.4. Anticoagulant activity assessment

Anticoagulant activity of furcellaran and its sulfated derivates was evaluated by their capacity to inhibit the clotting process and the results obtained are shown in **Fig. 4**. The clotting time of normal citrated

plasma as negative control in activated partial thromboplastin time ($aPTT$) thrombin time (PT) and prothrombin time (TT) assay was 27.7 s, 11.1 s and 18.2 s, respectively. These values are in compliance with the values stated for saline solution [**64-66**].

The activated partial thromboplastin time ($aPTT$) prolongation designates the inhibition of the intrinsic or common pathway. All the samples demonstrated a dose dependent prolongation of $aPPT$ at the concentration range of 0.1-2 mg/mL, except the sample FUR_DCC. Despite the higher sulfur content in comparison with native furcellaran, slight differences in proportions and/or distribution of sulfated residues along the galactan backbone may be responsible for the interaction between proteases, inhibitors, and activators of the coagulation system, inducing procoagulant action [**67**]. Thus, differences in the sulfation degree or sulfation pattern along the polysaccharide chain could be the reason for the results of FUR_DCC. The most active of tested samples was FUR_HSO3CL showing almost 4-fold higher anticoagulant activity than native furcellaran at the concentration 2 mg/mL. Samples FUR_DMSO and FUR_DMF showed at higher doses significant prolongation of clotting time (120.7 s and 120.3 s) as well. As expected, native furcellaran displayed elevated anticoagulant activity, which is consistent with previous studies devoted to carrageenans [**18,39,68**]. The results clearly indicate that the total sulfate content (as confirmed by $FT-IR$) is the major factor resulting in prolongation of $aPPT$. The study of X-carra-geenan even has increased anticoagulant activity if the molecular weight is substantially lower compared to the native sample, suggesting carrageenans might exhibit optimal efficacy within a certain molecular weight range [**69**]. The notable $aPPT$ time prolongation of native FUR underscores that its relatively high molecular weight may have greater chance of colliding effectively as the long-chain possesses more repeating units and higher valence to bind to more receptors [**70**].

The thrombin time (TT) assay was used to investigate the influence of polysaccharides on fibrin formation from fibrinogen in plasma. All samples excepting FUR_DCC retarded the time of clot formation in concentration dependent manner.

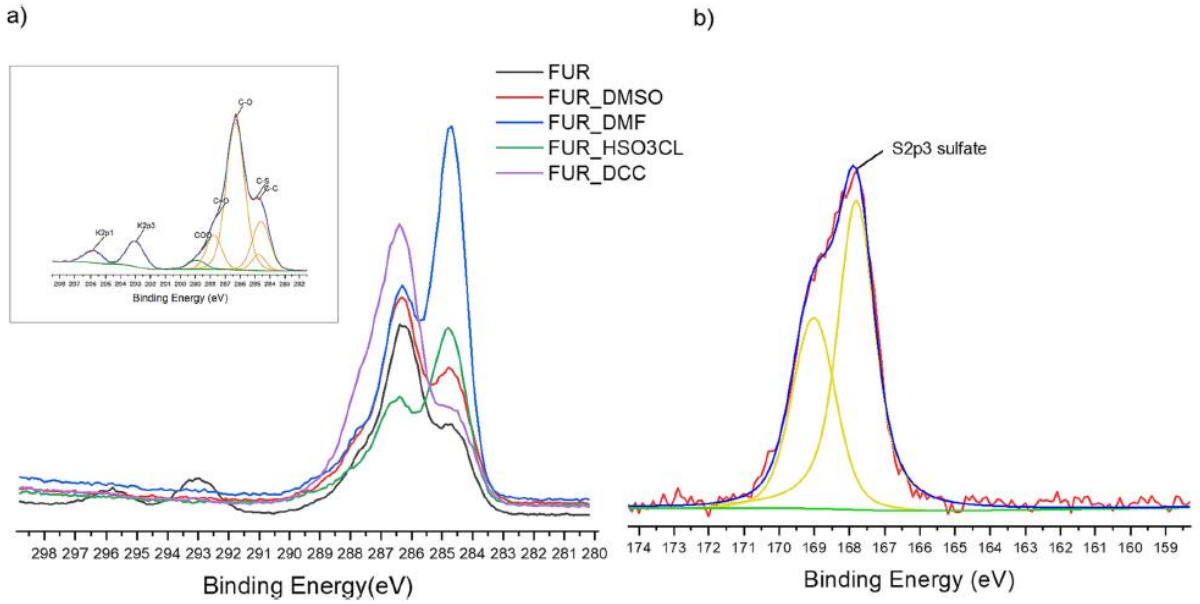

Fig. 3. XPS spectra: a) overlay of the high-resolution C 1s scans for furcellaran and its derivates. Inset displays the results of C 1s deconvolution for FUR sample, b) binding of sulfate.

Table 3 Elemental analysis of furcellaran and its derivates.

Sample	Elements (% w/w)					
	C	S	H	N	DS[a]	Yield (w/w %)
FUR	31.5 ± 0.4	2.0 ± 0.2	4.9 ± 0.3	0.1	0.15	–
FUR_DMSO	22.8 ± 0.1	8.0 ± 0.1	4.1 ± 0.2	1	0.8	84.1
FUR_DMF	21.7 ± 0.1	8.2 ± 0.3	4.2 ± 0.2	0.8	0.53	81.8
FUR_HSO3CL	16.8	6.9 ± 0.3	2.8	0.4	0.91	90.3
FUR_DCC	25.7 ± 0.2	3.2 ± 0.2	4.2	0.8	0.28	74.0

[a] *DS - degrees of sulfate substitution.*

Comparing the anticoagulant potencies of native furcellaran with sulfated derivates at the same concentration, it can be noted that the anticoagulant activity is independent of DS by showing similar values. It has been shown that anticoagulant activity of high molecular weight λ-carrageenan was higher in the thrombin time assay [**69**], which was also indicated by current results. Pomin and Mourao [**71**] stated that charge density and sulfate content are important parameters for anticoagulant action, however the overall structural features of SPs are still more influential for interaction with coagulation cofactors and their target proteases and inhibitors were determined to be very stereospecific. In addition, Liang and Maio [**39**] suggested, that the existence of sulfate ester at G4 position appeared to be more beneficial than at G6 position. Hence, chemical characteristics such as glycosidic linkage and sulfation pattern are also prerequisites for correlating the biological functions of these compounds.

The PT assay was used to investigate the effect on extrinsic pathway of coagulation. Among the all tested samples, FUR_HSO3CL showed itself to be the most potent anticoagulant agent in PT assay with time 16 s at a concentration 2 mg/mL. This might be contributed to the significant reduction of M_w (2.7 kDa) during the sulfated modification with high DS of the sample. The low molecular weight fractions from the sulfated galactan of Botryocladia occidentalis showed high anticoagulant activity, and the total thrombin inhibition mediated by the heparin cofactor II was even stronger that of the parent polysaccharide [**3**]. LMW fraction of 8 kDa derived from the fucoidan of A. nodosum reduced mean thrombus weight by 80 % vs control saline injection in rabbit model of venous thrombosis [**72**]. λ -carrageenan inhibited factor Xa or factor II exclusively in M_w <6 kDa. This suggests the direct antithrombin activity of oligosaccharide defined by sulfate pattern [**35**]. Other studies have shown oligosaccharides likely interact directly with the proteins of the coagulation cascades without potentiating the AT-II [**73,74**]. The clotting times of other oversulfated derivates were also slightly prolonged but still within the range of physiological values. On the contrary, native furcellaran showed no prolongation of prothrombin time, illustrating that inhibition of the extrinsic coagulation factors will largely depend on the sulfate content and partly on the molecular weight. Opoku et al. demonstrated that oversulfated K-carrageenan exhibited higher anticoagulant effect in doubling PT compared to a native one. Analogous trend was observed for fucoidan [**75**]. Thus, the effect on extrinsic pathway was observed as the weakest and suggested the action profile of samples was similar

to that of heparin. Heparin is known to inhibit coagulation cascade by catalyzing the factor Xa and thrombin neutralization by the endogenous coagulation inhibitor antithrombin [**76**].

Furcellaran and its oversulfated derivates may act only on the intrinsic pathways of the blood coagulation system, which is reflected in their insignificant prolongation of the clotting time in PT assay. In other words, samples did not have much influence on the inhibition on Factor III, but the anticoagulant activity mechanism can be shown via thrombin inhibition. The high DS could increase the negative charge density to inhibit the activity of IIa and Xa. $aPPT$ and TT assay also manifest that not only high density of sulfates, but also molecular size, position of sulfate groups and other structural features are important for the anticoagulant behavior. This conclusion was uniform with earlier studies. Although the anticoagulant activities of furcellaran and sulfated deri-vates were less potent than those of heparin, clotting of $aPPT$ and TT were considerably elevated at concentrations 0.1 mg/mL and above compared to negative saline control.

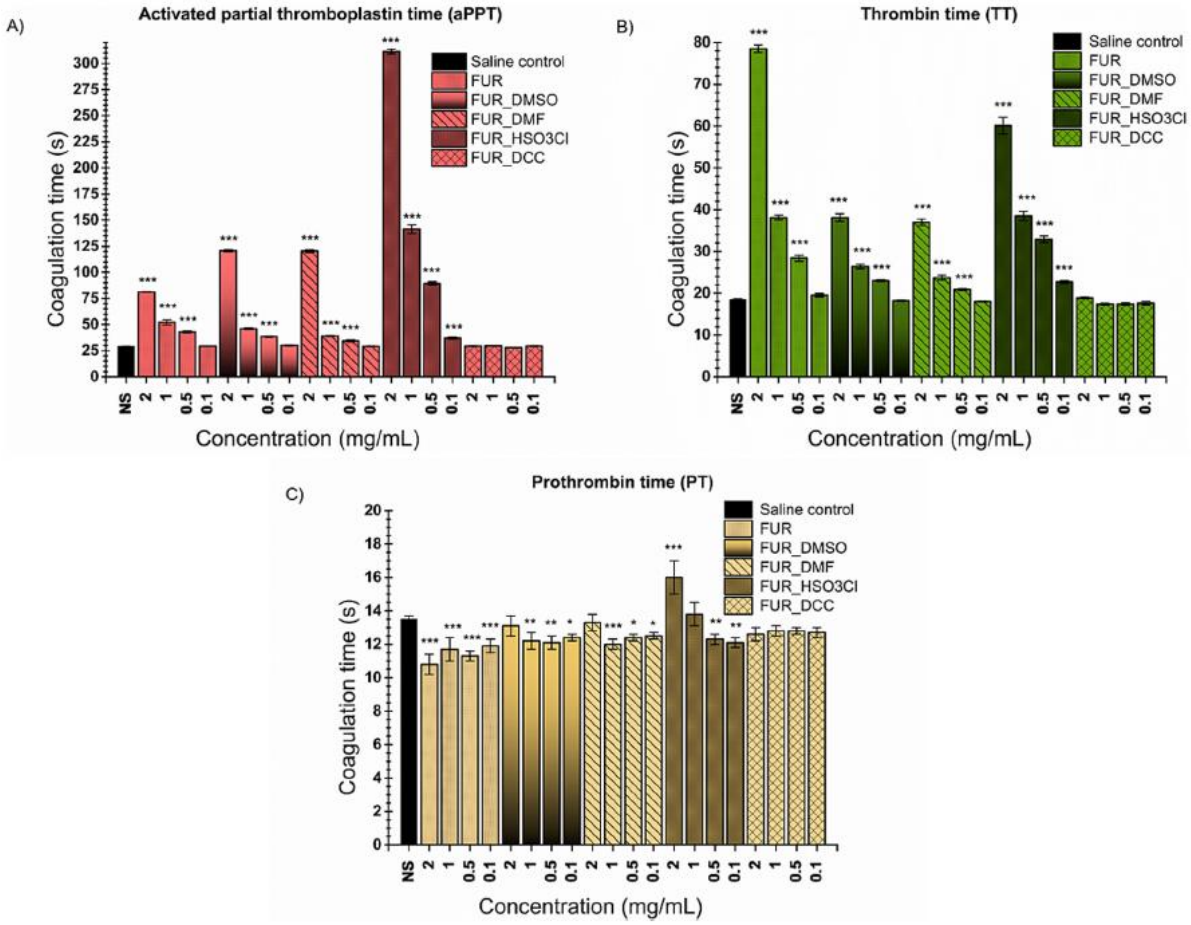

Fig. 4. Anticoagulation activity analysis of native furcellaran and its sulfated derivates using different coagulation assays: A) $aPTT$ (activated partial thromboplastin time); B) TT (thrombin time); C) PT (prothrombin time). The values are expressed as mean value $\pm SD$ of three independent tests ($n = 3$). Significant differences compared to the control group (NS: negative control, saline solution) are designated as $^{*}\ p < 0.05$; $^{**}\ p < 0.01$; $^{***}\ p < 0.001$. The clotting time of saline solution in the PT, $APTT$ and TT assays was 13.5 ± 0.2 s, 29.1 ± 0.1 s, and 18.5 ± 0.2 s, respectively. No coagulation response was observed for sodium heparin (positive control) across the range of concentrations tested.

3.5. In vitro fibroblast cytocompatibility

The cytotoxicity of native furcellaran and its oversulfated derivates at the range of concentrations 0.1-2 mg/mL was investigated, and the results obtained in triplicates are shown as the percentage of cell

viability. To calculate the cytotoxicity percentage of the sample, a negative control of polystyrene and cells in culture medium was used. As it is shown in **Fig. 5**, all tested samples decreased cell viability in a dose dependent manner while all of them are non-cytotoxic up to the concentration of 0.1 mg/mL. Compared to sulfated derivates, native furcellaran remained least cytotoxic, as the viability reached 76.8 % at the concentration of 1 mg/mL. With the increase of the concentration to 2 mg/mL, the significant reduction of viability was observed for all samples after 48 h of treatment. The previous study demonstrated that high DS (0.28-0.66) contribute to cytotoxicity more likely than DS with lower values (0.11-0.14) [**77**]. No direct relationship between the cytotoxic activity and DS values were observed among the oversulfated samples but it may be a decisive aspect influencing the higher viability in native furcellaran. Besides, SPs with high DS are mostly accompanied with lower M_w and changes in the original chain conformation resulted from strong acidic conditions. For SO_3•Py complex reaction, two different solvents, $DMSO$ and DMF were utilized to leverage their distinct nucleophilic properties to achieve varying degree of sulfation.

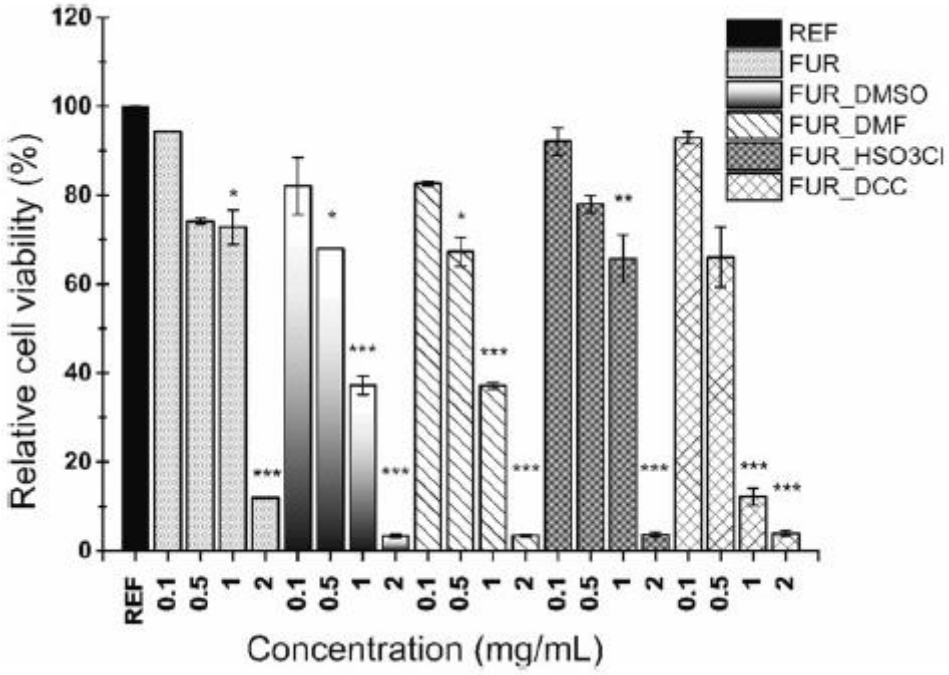

Fig. 5. Relative cell viability values expressed as a percent of control (expanded polystyrene). Values represent the mean of three test wells. Error bars represent standard deviations. Significant difference among groups was indicated as $^{*}\ p\ <0.05$, $^{**}\ p\ <0.01$, $^{***}\ p\ <0.001$.

Despite to presumed stronger nucleophilic ability and lower cell growth inhibition of $DMSO$ solvent [**37,78**], both FUR_DMSO and FUR_DMF samples demonstrated comparable cell viability outcomes. This observation implies that the cytotoxicity cannot be solely attributed to the solvent used; rather it could potentially be modulated by the toxic nature of reactants. As pointed out in $FT-IR$, the sulfate groups were introduced to galactose unit on G-6 position, meanwhile the native furcellaran consists of galactose with sulfate group at G-4 position. According to Liang et al. [**39**], the substitution position affects cell viability rather than the sulfation degree whereas the introduction of sulfate groups on G-6 position of sulfated agarose causes stronger cytotoxicity. The same study demonstrated a 2-fold decrease in HUVEC cell viability after treatment with the oversulfated κ-carrageenan (1 mg/mL) compared to unmodified K-carrageenan. There are earlier studies presenting the cytotoxic activity of K-carrageenan oligosaccharides [**79-81**]. Combination of high DS, the M_w reduction and sulfation position in comparison to the unmodified furcellaran could contribute to their higher cytotoxic action.

As expected, the presence of anionic ions would prevent the interactions between the furcellaran and the cells as the membrane surface is negatively charged.

3.6. Evaluation of platelet adhesion test

The platelet adhesion density and degree of platelet activation are the crucial indices to evaluate the thrombogenicity of biomaterials. Many studies supported the fact that coagulation a platelet adhesion are intricately related processes that may considerably affect each other. Based on this, platelet adhesion test was assessed. The presence and morphology of platelets adhered to the samples were estimated by SEM micrographs (**Fig. 6**) that reveal a clear difference between untreated PET sample and the treated ones. As expected, the untreated PET surface (**Fig. 6**a,c) shows activated blood platelets with a dendritic spreading, hyalomere and intermediate pseudopodia network (emphasized by white arrow) indicating a poor hemocompatibility [**82**]. Only some round-shaped platelets in non-activated form were observed on the surface after RF air plasma discharge activation (FUR_DC) (**Fig. 6**e). Such a phenomenon can be explained by the introduced oxygen functional groups and higher hydrophilicity of the surface. Hydrophilic surface is less favorable for the adsorption of proteins, the initiating event in the processes occurring when artificial surface is in contact with blood [**83**]. All further events, such as platelet adhesion and activation of coagulation are then determined by initially adsorbed protein layer. Fibrinogen, one of the most abundant plasma proteins, has been closely related to the surface induced thrombus formation [**84**]. A predominance of inactivated platelets of spherical shape without platelet aggregation was found on the surface treated with native furcellaran (**Fig. 6**f).

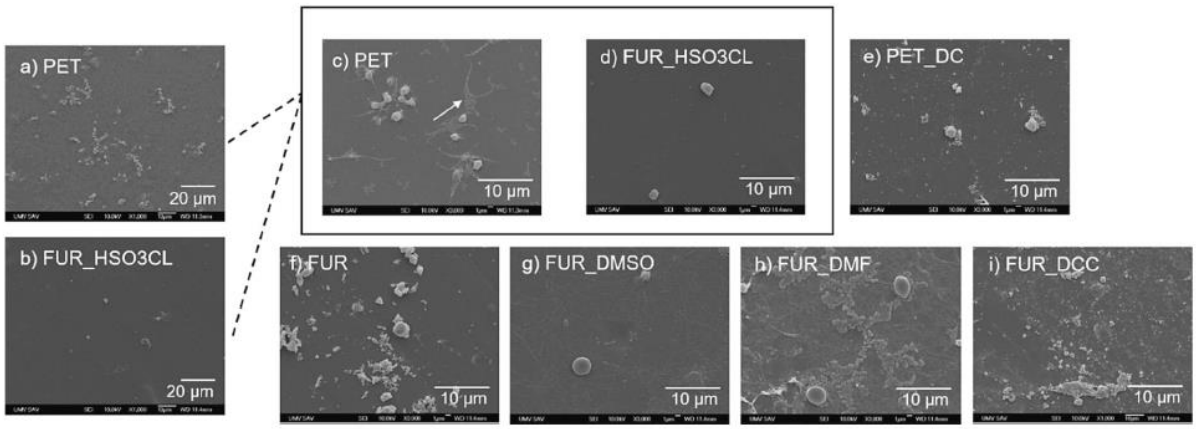

Fig. 6. Scanning Electron Microscope (SEM) micrographs for platelet adhesion assays on a) untreated PET, b) FUR_HSO3CL c) untreated PET, d) FUR_HSO3CL, e) Air plasma treated PET_DC, f) FUR, g) FUR_DMSO, h) FUR_DMF, i) FUR_DCC. Two different magnifications are shown: 1000 × (a, b) and 3000 × (c-i).

However, some undetectable particles were entrapped in the vicinity of platelets which may origin from the PRP itself. An optimal hemocompatible material will not adversely interact with any blood components so as to cause their inappropriate activation or even destruction. A similar case occurred on surface treated with FUR_DCC (**Fig. 6**i) and some platelet aggregates were also detected. These results suggest a poor antithrombotic property of the FUR_DCC sample since the platelet aggregation has long been recognized as critical for hemostatic plug formation and thrombosis [**85**]. This was also supported by the fact that sample FUR_DCC had no effect on coagulation process. In contrast, surfaces treated with highly sulfated furcellaran derivates (**Fig. 6**b,d,g-i) presented a significant decrease in platelet's adhesion, as well as absence of the most activated platelet stages on the pathway to full spreading. Sample FUR_DMSO (**Fig. 6**g) showed some resting platelets with discoid shape and

few inactivated spherical platelets indicating the excellent anti-platelets adhesion property and potential antithrombotic characteristics. Similar results were exhibited by the sample FUR_DMF (**Fig. 6**h), where platelets were trapped mainly around cracks of polysaccharide surface presumably caused during the dehydration process. For the sample FUR_HSO3CL (**Fig. 6**b,d), complete absence of activated platelets was observed, and platelet adhesion density became the lowest among the specimens studied. These results are consistent with data obtained from measurement of anticoagulant activity and might be associated with electrostatic repulsion of the negative charges promoted by the presence of sulfate groups [86]. Moreover, the hydrophilic properties of furcellaran surfaces provide the additive effect on antiplatelet activity [**87**].

4. Conclusions

In the present work, we proposed four sulfating methods for furcel-laran modification aiming to assess their distinctive impacts on hemo-compatibility. The obtained 6-O-sulfated furcellaran derivates varied in the degree of sulfation and were accompanied by low Mw. The incorporated sulfate esters were analyzed by $FTIR$, XPS and elemental analysis where the highest sulfate content was assigned to furcellaran sulfate prepared with chlorosulfonic acid and SO_3•Py complex in $DMSO$. Proportionally to the highest sulfate content and low M_w, sulfation via chlorosulfonic acid exhibited the most pronounced impact on the anticoagulant activity and showed the relevant antiplatelet effect. Furcel-laran sulfates produced by SO_3•Py complex showed significant influence particularly on the intrinsic and common pathway of the coagulation cascade, regardless of the solvent used and presented a significant decrease in platelet adhesion. SO_3•Py complex reagent resulted in noticeable sample degradation. However, its impact was comparatively milder than that observed with other methods. Particularly, $ClSO_3H$ generates harsh conditions that produce severe changes in the furcel-laran structure and alters the bioactivity of the sulfated derivatives significantly. However, even though the sulfation with excess of $ClSO_3H$ has led to partial hydrolysis, it proved to be an optimal reagent for sulfation of furcellaran. It was expected the sulfation with originating galactose-4-sulfate would lead to the anticipated formation of 4,6-disul-fated compound upon the introduction of a sulfate group at the 6-0 position [48]. Nevertheless, the observed result was confined to the formation of 0-6 sulfate, potentially suggesting the polysaccharide's susceptibility to solvolysis. Considering the position of galactose 4-sulfate in the context of its anticoagulant potential, native furcellaran was the most potent in retarding time of fibrin formation, indicating that not only sulfate content, but the general stereochemistry of the polysaccharide might be associated with the final step in the clotting cascade. Among all the obtained derivates, the one produced via dicy-clohexylcarbodiimide did not show any beneficial effect on anticoagulant nor antiplatelet action supposedly due to low sulfate pattern along with M_w. Consistent with other studies [**39,52**], sulfation also promoted dose-dependent cytotoxicity. These preliminary results provide strong evidence that the anticoagulant and antiplatelet potential of furcellaran is promoted by the sulfation and with further optimization it could broaden its range of potential applications not only with the biomedical field but also in areas such as environmental remediation and water treatment.

References

[1] D. Jiménez, B. Bikdeli, A. Quezada, A. Muriel, J.L. Lobo, J. de Miguel-Diez, L. Jara-Palomares, P. Ruiz-Artacho, R.D. Yusen, M. Monreal, Hospital volume and outcomes for acute pulmonary embolism: multinational population based cohort study, BMJ 366 (2019), l4416, **https://doi.org/10.1136/bmj.l4416**.

[2] E.I. Oduah, R.J. Linhardt, S.T. Sharfstein, Heparin: past, present, and future, Pharmaceuticals 9 (2016) 38, **https://doi.org/10.3390/ph9030038**.

[3] F.R. Melo, M.S. Pereira, D. Foguel, P.A.S. Mourao, Antithrombin-mediated anticoagulant activity of sulfated polysaccharides: different mechanisms for heparin and sulfated galactans, J. Biol. Chem. 279 (2004) 20824-20835, **https:// doi.org/10.1074/jbc.M308688200**.

[4] I. Bjork, U. Lindahl, Mechanism of the anticoagulant action of heparin, Mol. Cell. Biochem. 48 (1982) 161-182, **https://doi.org/10.1007/BF00421226**.

[5] A. Davenport, Review article: low-molecular-weight heparin as an alternative anticoagulant to unfractionated heparin for routine outpatient haemodialysis treatments, Nephrology 14 (2009) 455-461, **https://doi.org/10.1111/j.1440-1797.2009.01135.x**.

[6] A. Greinacher, Heparin-induced thrombocytopenia, N. Engl. J. Med. 373 (2015) 252-261, **https://doi.org/10.1056/NEJMcp1411910**.

[7] F.N. Croles, M.V. Lukens, R. Mulder, M.P.M. de Maat, A.B. Mulder, K. Meijer, Monitoring of heparins in antithrombin-deficient patients, Thromb. Res. 175 (2019) 8-12, **https://doi.org/10.1016/j.thromres.2019.01.007**.

[8] M.S. Arokiarajan, R. Thirunavukkarasu, J. Joseph, O. Ekaterina, W. Aruni, Advance research in biomedical applications on marine sulfated polysaccharide, Int. J. Biol. Macromol. 194 (2022) 870-881, **https://doi.org/10.1016/j.ijbiomac.2021.11.142**.

[9] Y. Yao, A.M. Zaw, D.E.J. Anderson, M.T. Hinds, E.K.F. Yim, Fucoidan functionalization on poly(vinyl alcohol) hydrogels for improved endothelialization and hemocompatibility, Biomaterials 249 (2020), 120011, **https://doi.org/ 10.1016/j.biomaterials.2020.120011**.

[10] K. Cui, W. Tai, X. Shan, J. Hao, G. Li, G. Yu, Structural characterization and antithrombotic properties of fucoidan from Nemacystus decipiens, Int. J. Biol. Macromol. 120 (2018) 1817-1822, **https://doi.org/10.1016/j. ijbiomac.2018.09.079**.

[11] F.D. da S. Chagas, G.C. Lima, V.I.N. dos Santos, L.E.C. Costa, W.M. de Sousa, V. G. Sombra, D.F. de Araújo, F.C.N. Barros, E. Marinho-Soriano, J.P. de Andrade Feitosa, R.C.M. de Paula, M.G. Pereira, A.L.P. Freitas, Sulfated polysaccharide from the red algae Gelidiella acerosa: anticoagulant, antiplatelet and antithrombotic effects, Int. J. Biol. Macromol. 159 (2020) 415-421, **https://doi.org/10.1016/j. ijbiomac.2020.05.012**.

[12] W.S.A. Mettwally, A.A. Gamal, N.G. Shams El-Din, A.A. Hamdy, Biological activities and structural characterization of sulfated polysaccharide extracted from a newly Mediterranean sea record Grateloupia gibbesii Harvey, Biocatal. Agricult. Biotechnol. 45 (2022), 102487, **https://doi.org/10.1016/j.bcab.2022.102487**.

[13] M. Khotimchenko, V. Tiasto, A. Kalitnik, M. Begun, R. Khotimchenko, E. Leonteva, I. Bryukhovetskiy, Y. Khotimchenko, Antitumor potential of carrageenans from marine red algae, Carbohydr. Polym. 246 (2020), 116568, **https://doi.org/ 10.1016/j.carbpol.2020.116568**.

[14] M. Alvarez-Vmas, S. Souto, N. Flárez-Fernández, M.D. Torres, I. Bandín, H. Dominguez, Antiviral activity of carrageenans and processing implications, Mar. Drugs 19 (2021) 437, **https://doi.org/10.3390/md19080437**.

[15] H.T. Ha, D.X. Cuong, L.H. Thuy, P.T. Thuan, D.T.T. Tuyen, V.T. Mo, D.H. Dong, Carrageenan of red algae Eucheuma gelatinae: extraction, antioxidant activity, rheology characteristics, and

physicochemistry characterization, Molecules 27 (2022) 1268, **https://doi.org/10.3390/molecules27041268**.

[16] A.A.S. de Sousa, N.M.B. Benevides, A. de Freitas Pires, F.P. Fiúza, M.G.R. Queiroz, T.M.F. Morais, M.G. Pereira, A.M.S. Assreuy, A report of a galactan from marine alga Gelidium crinale with in vivo anti-inflammatory and antinociceptive effects, Fundam. Clin. Pharmacol. 27 (2013) 173-180, **https://doi.org/10.1111/j.1472-8206.2011.01001.x**.

[17] H.M. Amaro, F. Pagels, T.G. Tavares, I. Costa, I. Sousa-Pinto, A.C. Guedes, Antioxidant and anti-inflammatory potential of seaweed extracts as functional ingredients, Hydrobiology 1 (2022) 469-482, **https://doi.org/10.3390/ hydrobiology1040028**.

[18] F.R.F. Silva, C.M.P.G. Dore, C.T. Marques, M.S. Nascimento, N.M.B. Benevides, H. A.O. Rocha, S.F. Chavante, E.L. Leite, Anticoagulant activity, paw edema and pleurisy induced carrageenan: action of major types of commercial carrageenans, Carbohydr. Polym. 79 (2010) 26-33, **https://doi.org/10.1016/j. carbpol.2009.07.010**.

[19] K.T. Kubra, Md.S. Salman, Md.N. Hasan, Enhanced toxic dye removal from wastewater using biodegradable polymeric natural adsorbent, J. Mol. Liq. 328 (2021), 115468, **https://doi.org/10.1016/j.molliq.2021.115468**.

[20] O. Duman, T.G. Polat, C.O. Diker, S. Tun^, Agar/K-carrageenan composite hydrogel adsorbent for the removal of Methylene Blue from water, Int. J. Biol. Macromol. 160 (2020) 823-835, **https://doi.org/10.1016/j.ijbiomac.2020.05.191**.

[21] Md.M. Hasan, Md.S. Salman, Md.N. Hasan, A.I. Rehan, M.E. Awual, A.I. Rasee, R. M. Waliullah, M.S. Hossain, K.T. Kubra, Md.C. Sheikh, Md.A. Khaleque, H. M. Marwani, A. Islam, Md.R. Awual, Facial conjugate adsorbent for sustainable Pb (II) ion monitoring and removal from contaminated water, Colloids Surf. A Physicochem. Eng. Asp. 673 (2023), 131794, **https://doi.org/10.1016/j. colsurfa.2023.131794**.

[22] P. Kersen, T. Paalme, L. Pajusalu, G. Martin, Biotechnological applications of the red alga Furcellaria lumbricalis and its cultivation potential in the Baltic Sea, Bot. Mar. 60 (2017) 207-218, **https://doi.org/10.1515/bot-2016-0062**.

[23] F. Weinberger, T. Paalme, S.A. Wikstrom, Seaweed resources of the Baltic sea, Kattegat and german and danish North sea coasts, Bot. Mar. 63 (2020) 61-72, **https://doi.org/10.1515/bot-2019-0019**.

[24] K. Laos, S.G. Ring, Note: characterisation of furcellaran samples from estonian Furcellaria lumbricalis (Rhodophyta), J. Appl. Phycol. 17 (2005) 461-464, **https:// doi.org/10.1007/s10811-005-1635-2**.

[25] R. Tuvikene, K. Truus, M. Robal, O. Volobujeva, E. Mellikov, T. Pehk, A. Kollist, T. Kailas, M. Vaher, The extraction, structure, and gelling properties of hybrid galactan from the red alga Furcellaria lumbricalis (Baltic Sea, Estonia), J. Appl. Phycol. 22 (2010) 51-63, **https://doi.org/10.1007/s10811-009-9425-x**.

[26] V. Kůrová, R.N. Salek, M. Černíková, E. Lorencová, L. Zalesáková, F. Bunka, Furcellaran as a substitute for emulsifying salts in processed cheese spread and the resultant storage changes, Int. J. Dairy Technol. 75 (2022) 679-689, **https://doi. org/10.1111/1471-0307.12871**.

[27] L. Marangoni Júnior, R.P. Vieira, E. Jamráz, Č.A.R. Anjos, Furcellaran: an innovative biopolymer in the production of films and coatings, Carbohydr. Polym. 252 (2021), 117221, **https://doi.org/10.1016/j.carbpol.2020.117221**.

[28] V. Milosavljevic, E. Jamroz, M. Gagic, Y. Haddad, H. Michalkova, R. Balkova, B. Tesarova, A. Moulick, Z. Heger, L. Richtera, P. Kopel, V. Adam, Encapsulation of doxorubicin in furcellaran/chitosan nanocapsules by layer-by-layer technique for selectively controlled drug delivery, Biomacromolecules 21 (2020) 418-434, **https://doi.org/10.1021/acs.biomac.9b01175**.

[29] K. Stepánkova, K. Ozaltin, J. Pelková, H. Pičtčková, I. Karakurt, S. Kačerová, M. Lehocky, P. Humpolicek, A. Vesel, M. Mozetic, Furcellaran surface deposition and its potential in biomedical applications, Int. J. Mol. Sci. 23 (2022) 7439, **https://doi.org/10.3390/ijms23137439**.

[30] Y. Xu, Y.-J. Wu, P.-L. Sun, F.-M. Zhang, R.J. Linhardt, A.-Q. Zhang, Chemically modified polysaccharides: synthesis, characterization, structure activity relationships of action, Int. J. Biol. Macromol. 132 (2019) 970-977, **https://doi. org/10.1016/j.ijbiomac.2019.03.213**.

[31] W. Liu, H. Wang, W. Yao, X. Gao, L. (Lucy) Yu, Effects of sulfation on the physicochemical and functional properties of a water-insoluble polysaccharide preparation from Ganoderma lucidum, J. Agric. Food Chem. 58 (2010) 3336-3341, **https://doi.org/10.1021/jf903395g**.

[32] C. Liu, H. Chen, K. Chen, Y. Gao, S. Gao, X. Liu, J. Li, Sulfated modification can enhance antiviral activities of Achyranthes bidentata polysaccharide against porcine reproductive and respiratory syndrome virus (PRRSV) in vitro, Int. J. Biol. Macromol. 52 (2013) 21-24, **https://doi.org/10.1016/j.ijbiomac.2012.09.020**.

[33] J. Wang, A. Bao, Q. Wang, H. Guo, Y. Zhang, J. Liang, W. Kong, J. Yao, J. Zhang, Sulfation can enhance antitumor activities of Artemisia sphaerocephala polysaccharide in vitro and vivo, Int. J. Biol. Macromol. 107 (2018) 502-511, **https://doi.org/10.1016/j.ijbiomac.2017.09.018**.

[34] A. Chaidedgumjorn, H. Toyoda, E.R. Woo, K.B. Lee, Y.S. Kim, T. Toida, T. Imanari, Effect of (1^3)- and (1^4)-linkages of fully sulfated polysaccharides on their anticoagulant activity, Carbohydr. Res. 337 (2002) 925-933, **https://doi.org/ 10.1016/S0008-6215(02)00078-2**.

[35] H. Groult, R. Cousin, C. Chot-Plassot, M. Maura, N. Bridiau, J.-M. Piot, T. Maugard, I. Fruitier-Arnaudin, X-Carrageenan oligosaccharides of distinct anti-heparanase and anticoagulant activities inhibit MDA-MB-231 breast cancer cell migration, Mar. Drugs 17 (2019) 140, **https://doi.org/10.3390/md17030140**.

[36] C.A. de Araujo, M.D. Noseda, T.R. Cipriani, A.G. Gonsalves, M.E.R. Duarte, D.R. B. Ducatti, Selective sulfation of carrageenans and the influence of sulfate regiochemistry on anticoagulant properties, Carbohydr. Polym. 91 (2013) 483-491, **https://doi.org/10.1016/j.carbpol.2012.08.034**.

[37] J. Yang, Y. Du, Y. Wen, T. Li, L. Hu, Sulfation of Chinese lacquer polysaccharides in different solvents, Carbohydr. Polym. 52 (2003) 397-403, **https://doi.org/ 10.1016/S0144-8617(02)00330-2**.

[38] Y. Jie, L. Zhang, P. Chen, X. Mao, S. Tang, Preparation of agarose sulfate and its antithrombogenicity, J. Wuhan Univ. Technol.-Mat. Sci. Edit. 27 (2012) 110-114, **https://doi.org/10.1007/s11595-012-0418-2**.

[39] W. Liang, X. Mao, X. Peng, S. Tang, Effects of sulfate group in red seaweed polysaccharides on anticoagulant activity and cytotoxicity, Carbohydr. Polym. 101 (2014) 776-785, **https://doi.org/10.1016/j.carbpol.2013.10.010**.

[40] E. Bedini, A. Laezza, M. Parrilli, A. Iadonisi, A review of chemical methods for the selective sulfation and desulfation of polysaccharides, Carbohydr. Polym. 174 (2017) 1224-1239, **https://doi.org/10.1016/j.carbpol.2017.07.017**.

[41] A.F.D. Vasconcelos, R.F.H. Dekker, A.M. Barbosa, E.R. Carbonero, J.L.M. Silveira, B. Glauser, M.S. Pereira, M. de L. Corradi da Silva, Sulfonation and anticoagulant activity of fungal exocellular p-(1^6)-d-glucan (lasiodiplodan), Carbohydr. Polym. 92 (2013) 1908-1914, **https://doi.org/10.1016/j.carbpol.2012.10.034**.

[42] H.P. de Oliveira Barddal, A.H.P. Gracher, F.F. Simas-Tosin, M. Iacomini, T. R. Cipriani, Anticoagulant activity of native and partially degraded glycoglucuronomannan after chemical sulfation, Int. J. Biol. Macromol. 80 (2015) 328-333, **https://doi.org/10.1016/j.ijbiomac.2015.06.051**.

[43] A.H.P. Gracher, A.G. Santana, T.R. Cipriani, M. Iacomini, A procoagulant chemically sulfated mannan, Carbohydr. Polym. 136 (2016) 177-186, **https://doi. org/10.1016/j.carbpol.2015.09.022**.

[44] H. Guo, H.-Y. Li, L. Liu, C.-Y. Wu, H. Liu, L. Zhao, Q. Zhang, Y.-T. Liu, S.-Q. Li, W. Qin, D.-T. Wu, Effects of sulfated modification on the physicochemical properties and biological activities of p-glucans from Qingke (Tibetan hulless barley), Int. J. Biol. Macromol. 141 (2019) 41-50, **https://doi.org/10.1016/j. ijbiomac.2019.08.245**.

[45] H. Li, X. Wang, Q. Xiong, Y. Yu, L. Peng, Sulfated modification, characterization, and potential bioactivities of polysaccharide from the fruiting bodies of Russula virescens, Int. J. Biol. Macromol. 154 (2020) 1438-1447, **https://doi.org/10.1016/ j.ijbiomac.2019.11.025**.

[46] M. Tengdelius, C.-J. Lee, M. Grenegård, M. Griffith, P. Páhlsson, P. Konradsson, Synthesis and biological evaluation of fucoidan-mimetic glycopolymers through cyanoxyl-mediated free-radical polymerization, Biomacromolecules 15 (2014) 2359-2368, **https://doi.org/10.1021/bm5002312**.

[47] R. Takano, S. Yoshikawa, T. Ueda, K. Hayashi, S. Hirase, S. Hara, Sulfation of polysaccharides with sulfuric acid mediated by dicyclohexylcarbodiimide, J. Carbohydr. Chem. 15 (1996) 449-457, **https://doi.org/10.1080/ 07328309608005665**.

[48] G. Opoku, X. Qiu, V. Doctor, Effect of oversulfation on the chemical and biological properties of kappa carrageenan, Carbohydr. Polym. 65 (2006) 134-138, **https:// doi.org/10.1016/j.carbpol.2005.12.033**.

[49] J.M. Kim, I.-H. Bae, K.S. Lim, J.-K. Park, D.S. Park, S.-Y. Lee, E.-J. Jang, M.S. Ji, D. S. Sim, Y.J. Hong, Y. Ahn, J.C. Park, J.G. Cho, J.C. Kang, I.-S. Kim, M.H. Jeong, A method for coating fucoidan onto bare metal stent and in vivo evaluation, Prog. Org. Coat. 78 (2015) 348-356, **https://doi.org/10.1016/j.porgcoat.2014.07.013**.

[50] N. Shanthi, P. Arumugam, M. Murugan, M.P. Sudhakar, K. Arunkumar, Extraction of fucoidan from Turbinaria decurrens and the synthesis of fucoidan-coated AgNPs for anticoagulant application, ACS Omega 6 (2021) 30998-31008, **https://doi.org/ 10.1021/acsomega.1c03776**.

[51] **A. Kolender, C.A. Pujol, E. Damonte, A. Cerezo, M. Matulewicz, Sulfation of kappa-carrageenan and antiviral activity, in: Anales Des La Asociacion Quimica Argentina vol. 86, 1998, pp. 304-311**.

[52] F.T.G.S. Cardozo, C.M. Camelini, M.N.S. Cordeiro, A. Mascarello, B.G. Malagoli, I. v. Larsen, M.J. Rossi, R.J. Nunes, F.C. Braga, C.R. Brandt, C.M.O. Simoes, Characterization and cytotoxic activity of sulfated derivatives of polysaccharides from Agaricus brasiliensis, Int. J. Biol. Macromol. 57 (2013) 265-272, **https://doi. org/10.1016/j.ijbiomac.2013.03.026**.

[53] Eá. de Moura Neto, J. da S. Maciel, P.L.R. Cunha, R.C.M. de Paula, J.P.A. Feitosa, Preparation and characterization of a chemically sulfated cashew gum polysaccharide, J. Braz. Chem. Soc. 22 (2011) 1953-1960, **https://doi.org/ 10.1590/S0103-50532011001000017**.

[54] S. Gunasekaran, S. Govindan, P. Ramani, Sulfated modification, characterization and bioactivities of an acidic polysaccharide fraction from an edible mushroom Pleurotus eous (Berk.) Šacc, Heliyon 7 (2021), **https://doi.org/10.1016/j. heliyon.2021.e05964**.

[55] K. Ozaltin, M. Lehocky, P. Humpolicek, J. Pelkova, A. Di Martino, I. Karakurt, P. Saha, Anticoagulant polyethylene terephthalate surface by plasma-mediated fucoidan immobilization, Polymers 11 (2019) 750, **https://doi.org/10.3390/ polym11050750**.

[56] N.A.A. Ghani, R. Othaman, A. Ahmad, F.H. Anuar, N.H. Hassan, Impact of purification on iota carrageenan as solid polymer electrolyte, Arab. J. Chem. 12 (2019) 370-376, **https://doi.org/10.1016/j.arabjc.2018.06.008**.

[57] L.D. Hung, H.T.T. Nguyen, V.T.D. Trang, Kappa carrageenan from the red alga Kappaphycus striatus cultivated at Vanphong Bay, Vietnam: physicochemical properties and structure, J. Appl. Phycol. 33 (2021) 1819-1824, **https://doi.org/ 10.1007/s10811-021-02415-1**.

[58] J. Cotas, V. Marques, M.B. Afonso, C.M.P. Rodrigues, L. Pereira, Antitumour potential of Gigartina pistillata carrageenans against colorectal cancer stem cell-enriched tumourspheres, Mar. Drugs 18 (2020) 50, **https://doi.org/10.3390/ md18010050**.

[59] B. Matsuhiro, Vibrational spectroscopy of seaweed galactans, Hydrobiologia 326 (1996) 481-489, **https://doi.org/10.1007/BF00047849**.

[60] X.-T. Xie, X. Zhang, Y. Liu, X.-Q. Chen, K.-L. Cheong, Quantification of 3,6-anhy-dro-galactose in red seaweed polysaccharides and their potential skin-whitening activity, 3 Biotech. 10 (2020) 189, **https://doi.org/10.1007/s13205-020-02175-8**.

[61] J. Prado-Fernáandez, J.A. Rodríguez-Váazquez, E. Tojo, J.M. Andrade, Quantitation of K-, i- and X-carrageenans by mid-infrared spectroscopy and PLS regression, Anal. Chim. Acta 480 (2003) 23-37, **https://doi.org/10.1016/S0003-2670(02)01592-1**.

[62] H. Vogl, D.H. Paper, G. Franz, Preparation of a sulfated linear (1^4)-P-d-galactan with variable degrees of sulfation, Carbohydr. Polym. 41 (2000) 185-190, **https:// doi.org/10.1016/S0144-8617(99)00076-4**.

[63] J. Yang, K. Luo, D. Li, S. Yu, J. Cai, L. Chen, Y. Du, Preparation, characterization and in vitro anticoagulant activity of highly sulfated chitosan, Int. J. Biol. Macromol. 52 (2013) 25-31, **https://doi.org/10.1016/j.ijbiomac.2012.09.027**.

[64] C. Bian, Z. Wang, J. Shi, Extraction optimization, structural characterization, and anticoagulant activity of acidic polysaccharides from Auricularia auricula-judae, Molecules 25 (2020) 710, **https://doi.org/10.3390/molecules25030710**.

[65] J. Zhao, J. Yang, S. Song, D. Zhou, W. Qiao, C. Zhu, S. Liu, B. Zhu, Anticoagulant activity and structural characterization of polysaccharide from Abalone (Haliotis discus hannai Ino) gonad, Molecules 21 (2016) 697, **https://doi.org/10.3390/ molecules21060697**.

[66] M. Dhahri, S. Sioud, R. Dridi, M. Hassine, N.A. Boughattas, F. Almulhim, Z. Al Talla, M. Jaremko, A.-H.M. Emwas, Extraction, characterization, and anticoagulant activity of a sulfated polysaccharide from Bursatella leachii viscera, ACS Omega 5 (2020) 14786-14795, **https://doi.org/10.1021/acsomega.0c01724**.

[67] R.J.C. Fonseca, S.-N.M.C.G. Oliveira, F.R. Melo, M.G. Pereira, N.M.B. Benevides, P. A.S. Mouraoo, Slight differences in sulfation of algal galactans account for differences in their anticoagulant and venous antithrombotic activities, Thromb. Haemost. 99 (2008) 539-545, **https://doi.org/10.1160/TH07-10-0603**.

[68] E.V. Sokolova, A.O. Byankina, A.A. Kalitnik, Y.H. Kim, L.N. Bogdanovich, T. F. Solov'eva, I.M. Yermak, Influence of red algal sulfated polysaccharides on blood coagulation and platelets activation in vitro, J. Biomed. Mater. Res. A 102 (2014) 1431-1438, **https://doi.org/10.1002/jbm.a.34827**.

[69] K. Saluri, R. Tuvikene, Anticoagulant and antioxidant activity of lambda- and theta-carrageenans of different molecular weights, Bioact. Carbohydr. Diet. Fibre 24 (2020), 100243, **https://doi.org/10.10Wj.bcdf.2020.100243**.

[70] M.Y.K. Leung, C. Liu, J.C.M. Koon, K.P. Fung, Polysaccharide biological response modifiers, Immunol. Lett. 105 (2006) 101-114, **https://doi.org/10.1016/). imlet.2006.01.009**.

[71] V.H. Pomin, P.A.S. Mouráo, Specific sulfation and glycosylation—a structural combination for the anticoagulation of marine carbohydrates, Front. Cell. Infect. Microbiol. 4 (2014) 33, **https://doi.org/10.3389/fcimb.2014.00033**.

[72] J. Millet, S.C. Jouault, S. Mauray, J. Theveniaux, C. Sternberg, B.C. Vidal, A. M. Fischer, Antithrombotic and anticoagulant activities of a low molecular weight fucoidan by the subcutaneous route, Thromb. Haemost. 81 (1999) 391-395, **https://doi.org/10.1055/s-0037-1614484**.

[73] K. Matsubara, Y. Matsuura, A. Bacic, M.-L. Liao, K. Hori, K. Miyazawa, Anticoagulant properties of a sulfated galactan preparation from a marine green alga,Codium cylindricum, Int. J. Biol. Macromol. 28 (2001) 395-399, **https://doi. org/10.1016/S0141-8130(01)00137-4**.

[74] P.V. Fernández, I. Quintana, A.S. Cerezo, J.J. Caramelo, L. Pol-Fachin, H. Verli, J. M. Estevez, M. Ciancia, Anticoagulant activity of a unique sulfated pyranosic (W3)-P-l-arabinan through direct interaction with thrombin, J. Biol. Chem. 288 (2013) 223-233, **https://doi.org/10.1074/jbc.M112.386441**.

[75] X. Qiu, A. Amarasekara, V. Doctor, Effect of oversulfation on the chemical and biological properties of fucoidan, Carbohydr. Polym. 63 (2006) 224-228, **https:// doi.org/10.1016/j.carbpol.2005.08.064**.

[76] C.J. Lee, J.E. Ansell, Direct thrombin inhibitors, Br. J. Clin. Pharmacol. 72 (2011) 581-592, **https://doi.org/10.1111/j.1365-2125.2011.03916.x**.

[77] H. Bao, W.-S. Choi, S. You, Effect of sulfated modification on the molecular characteristics and biological activities of polysaccharides from Hypsizigus marmoreus, Biosci. Biotechnol. Biochem. 74 (2010) 1408-1414, **https://doi.org/ 10.1271/bbb.100076**.

[78] L. Jamalzadeh, H. Ghafoori, R. Sariri, H. Rabuti, J. Nasirzade, H. Hasani, M. R. Aghamaali, Cytotoxic effects of some common organic solvents on MCF-7, RAW-264.7 and human umbilical vein endothelial cells, Avicenna J. Med. Biochem. 4 (2016) 10-33453, **https://doi.org/10.17795/ajmb-33453**.

[79] H. Yuan, J. Song, Preparation, structural characterization and in vitro antitumor activity of kappa-carrageenan oligosaccharide fraction from Kappaphycus striatum, J. Appl. Phycol. 17 (2005) 7-13, **https://doi.org/10.1007/s10811-005-5513-8**.

[80] S.H.Z. Ariffin, W.W. Yeen, I.Z.Z. Abidin, R.M. Abdul Wahab, Z.Z. Ariffin, S. Senafi, Cytotoxicity effect of degraded and undegraded kappa and iota carrageenan in human intestine and liver cell lines, BMC Complement. Altern. Med. 14 (2014) 508, **https://doi.org/10.1186/1472-6882-14-508**.

[81] G.H. Calvo, V.A. Cosenza, D.A. Sáaenz, D.A. Navarro, C.A. Stortz, M.A. Cáespedes, L. A. Mamone, A.G. Casas, G.M. Di Venosa, Disaccharides obtained from carrageenans as potential antitumor agents, Sci. Rep. 9 (2019) 6654, **https://doi. org/10.1038/s41598-019-43238-y**.

[82] S.L. Goodman, Sheep, pig, and human platelet-material interactions with model cardiovascular biomaterials, J. Biomed. Mater. Res. 45 (1999) 240-250, **https:// doi.org/10.1002/(sici)1097-4636(19990605)45:3<240::aid-jbm12>3.0.co;2-c.**

[83] Z.-K. Kuo, M.-Y. Fang, T.-Y. Wu, T. Yang, H.-W. Tseng, C.-C. Chen, C.-M. Cheng, Hydrophilic films: how hydrophilicity affects blood compatibility and cellular compatibility, Adv. Polym. Technol. 37 (2018) 1635-1642, **https://doi.org/ 10.1002/adv.21820**.

[84] B. Sivaraman, R.A. Latour, The relationship between platelet adhesion on surfaces and the structure versus the amount of adsorbed fibrinogen, Biomaterials 31 (2010) 832-839, **https://doi.org/10.1016/j.biomaterials.2009.10.008**.

[85] S.P. Jackson, The growing complexity of platelet aggregation, Blood 109 (2007) 5087-5095, **https://doi.org/10.1182/blood-2006-12-027698**.

[86] J.B.M. Rocha Neto, F. Copes, P. Chevallier, R.S. Vieira, J.V.L. da Silva, D. Mantovani, M.M. Beppu, Polysaccharide-based layer-by-layer nanoarchitectonics with sulfated chitosan for tuning anti-thrombogenic properties, Colloids Surf. B: Biointerfaces 213 (2022), 112359, **https://doi.org/10.1016/j. colsurfb.2022.112359**.

[87] P.K. Thalla, H. Fadlallah, B. Liberelle, P. Lequoy, G. De Crescenzo, Y. Merhi, S. Lerouge, Chondroitin sulfate coatings display low platelet but high endothelial cell adhesive properties favorable for vascular implants, Biomacromolecules 15 (2014) 2512-2520, **https://doi.org/10.1021/bm5003762**.